



LJMU Research Online

Dong, M, Ma, H, Zhang, G, Chen, Y, Zhang, X and Cao, X

A model for determining electromechanical response profile of ultrasonic transducers and ultrasonic transient echo

<http://researchonline.ljmu.ac.uk/id/eprint/8001/>

Article

Citation (please note it is advisable to refer to the publisher's version if you intend to cite from this work)

Dong, M, Ma, H, Zhang, G, Chen, Y, Zhang, X and Cao, X (2017) A model for determining electromechanical response profile of ultrasonic transducers and ultrasonic transient echo. Shengxue Xuebao/Acta Acustica, 42 (4). pp. 403-410. ISSN 0371-0025

LJMU has developed **LJMU Research Online** for users to access the research output of the University more effectively. Copyright © and Moral Rights for the papers on this site are retained by the individual authors and/or other copyright owners. Users may download and/or print one copy of any article(s) in LJMU Research Online to facilitate their private study or for non-commercial research. You may not engage in further distribution of the material or use it for any profit-making activities or any commercial gain.

The version presented here may differ from the published version or from the version of the record. Please see the repository URL above for details on accessing the published version and note that access may require a subscription.

For more information please contact researchonline@ljmu.ac.uk

<http://researchonline.ljmu.ac.uk/>

A model for determining electromechanical response profile of ultrasonic transducers and ultrasonic transient echo*

DONG Ming^{1,2†} MA Hongwei¹ ZHANG Guangming^{1,3} CHEN Yuan⁴ ZHANG Xuhui¹ CAO Xiangang¹

(1 School of Mechanical Engineering, Xi'an University of Science and Technology Xi'an 710054)

(2 Key Laboratory of Expressway Construction Machinery of Shaanxi Province, Chang'an University Xi'an 710054)

(3 General Engineering Research Institute, Liverpool John Moores University Liverpool L3 3AF)

(4 School of Science, Xi'an University of Science and Technology Xi'an 710054)

Abstract Models for calculating the radiation, scattering and reception of ultrasound are developed to provide a good understanding of the physical essence of ultrasonic testing. The process of ultrasonic wave generating by pulse, propagation in the medium and received by the transducer is analyzed, and the received ultrasonic signal can be found by convolving of the electromechanical response of transducer with the flaw impulse response. A model is proposed to predict the echo response from a plane defect based on the Huygens' principle of superposition. Spatial impulse response and Kirchhoff approximation are applied to model the interaction of the ultrasonic wave with flaws. The electromechanical response profile of transducer is calculated by deconvolution the echo of plane test block with impulse response of the test block. Characteristics of flaw impulse response of targets on and off-axis are analyzed in detail, the received ultrasonic echo is explained in terms of the plane and edge echoes, however, polarity is opposite. The amplitude of the direct echo is far greater than the edge echo. The theoretically predicted results are in good agreement with the experimentally results.

PACS numbers: 43.35, 43.38

1 Introduction

Ultrasonic pulse echo techniques are used in a wide variety of applications in nondestructive testing [1-2]. Ultrasonic modeling of acoustic field and flaw scattering is very helpful for explicit physical interpretations of the results of measurements, optimal transducer design and measurement system arrangement [3-5].

Flaw echo are often based on the characteristic of transducer and the geometry of the targets. An electromechanical characteristic of transfer function is associated with transducer for both the electromechanical response for transmit and receive ultrasonic signal [6]. The active element of most acoustic transducers used today is a piezoelectric ceramic, the difference in piezoelectric parameter of such material will be risen due to the high frequency vibration and depolarization trend [7-8]. Each transducer used is characterized by a specific response profile which must be included in the echo model. Several methods to calculate the response profile of transducer has been proposed. Flávio Buiochi [9] acquired the transducer response function by a 0.6-mm-diameter needle hydrophone placed approximately 5 mm from the transducer face, but the signal was disturbed by the edge wave. Jenson [10] used the reflected pulse of a perspex plate placing at the focal point as transducer response, and the response was filtered in the frequency domain by removing all components above 7MHz. For a focusing aperture, Szabo [11] show the reference waveform from a flat-plate target in the focal plane of a strongly focusing transducer (pressure focal grain is greater than 16) is appropriate to determine without distortion, and a point scatter is double time differential of the flat plate response. Demirli [12] and Boßmann Florian [13] developed a general Gaussian echo model whose parameters can be estimated iteratively. Wei Liang [14] used matching pursuit (MP) method to analyze noisy ultrasonic pulse-echo wavelet and decompose the noisy pulse-echo wavelet into unit-norm vectors, and the approximation transducer response was obtained. Roberto [15] used a regularization of

the Wiener filter to estimate of the transducer response. All of these results in [12]- [15] is inaccurate.

In this study, a model for determining electromechanical response profile of ultrasonic transducers from a plane defect based on the Huygens' principle of superposition is proposed. Spatial impulse response and Kirchoff approximation are applied to model the interaction of the ultrasonic wave with flaws. The electromechanical response profile of transducer is calculated by deconvolution the echo of plane test block with impulse response of the test block. Characteristics of flaw impulse response of targets on and off-axis are analyzed in detail, the received ultrasonic echo is explained in terms of the plane and edge echoes, however, polarity is opposite. The amplitude of the direct echo is far greater than the edge echo. The theoretically predicted results are in good agreement with the experimentally results.

2 Model of transducer response

2.1 Convolutional model of ultrasonic echo

Typically an ultrasonic echo signal transmission model can be expressed as follows: Following excitation by an electrical impulse, a transducer transmits an ultrasonic pulse into a sample, the ultrasonic pulse then propagates inside the test sample and can be reflected by some interface or crack in the sample. Next, the echo signal is transmitted back to the transducer and produces an electrical signal in the receiver. The transmission model is illustrated in Fig.1. The ultrasound echo can be described by a convolution formula as[16]

$$y(t) = p(t) * h_i(t) * h_{m1}(t) * h_s(t) * h_{m2}(t) * h_r(t) * h_i(t) \quad (1)$$

where $*$ denotes the convolution operation, $y(t)$ is the electrical signal received by the measurement system, $p(t)$ is the excitation impulse, $h_i(t)$ and $h_r(t)$ are the coefficients of electro-mechanical and mechanical-electrical transformation of the transducer, $h_{m1}(t)$ and $h_{m2}(t)$ are the forward and backward transfer characteristic functions of the couple medium and test sample, $h_s(t)$ is the impulse response of crack or interface, $h_i(t)$ is the characteristic functions of measurement system.

We define

$$v(t) = p(t) * h_i(t) * h_r(t) * h_i(t) \quad (2)$$

$$h(t) = h_s(t) * h_{m1}(t) * h_{m2}(t) \quad (3)$$

so Eq.(1) can be written as

$$y(t) = v(t) * h(t) \quad (4)$$

where $v(t)$ denote the transducer response, and $h(t)$ denote the characteristic functions of the inspected sample.

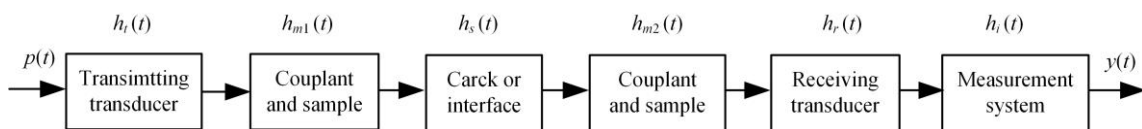


Fig.1 Ultrasound transmission model

2.2 Transducer response calculation

We carried out experiments to calculate transducer response by deconvolution the echo of plane test block with impulse response of the test block. The test block is homogeneous and free from cracks, and the coupling efficiency is good, $h_{m1}(t)$ and $h_{m2}(t)$ are ignored. So Eq.(3) can be rewritten as

$$h(t) = h_s(t) \quad (5)$$

The electrical signal received by the measurement system can be expressed as

$$y(t) = v(t) * h_s(t) \quad (6)$$

We assume the reflect echo from the back surface of the planar test block is $y_p(t)$, the impulse response of the test block is $h_p(t)$ which is calculated by a echo model. The Wiener inverse filter is used to estimate $v(t)$, and is written as

$$v(t) = \text{IFFT}\left(\frac{Y_p(\omega)H_p(\omega)^*}{|H_p(\omega)|^2 + Q^2}\right) \quad (7)$$

where $\text{IFFT}(\cdot)$ is Fourier inversion, $H_p(\omega)$ is frequency domain signals of $h_p(t)$, Q a priori SNR of the measurement system.

2.3 Model for interaction of ultrasound and flaw

The theoretical study is based on the ultrasound propagation in a lossless, homogeneous medium and on the hypothesis of linear acoustic. As shown in Fig.2, the flaw and receiving transducer is divided into rectangles elements. First, the velocity potential impulse response is calculated in each of the elementary areas of the flaw using the Rayleigh integral. Second, the reflected velocity potential impulse response is calculated by applying the Kirchhoff approximation. Finally, the acoustic pressure over the surface of the receiving transducer is calculated by applying Huygen's principle.

The theoretical concepts are based on the spatial impulse response, the velocity potential impulse response at point \mathbf{r}_f is given by

$$\phi(\mathbf{r}_f, t) = \int_{S_i} \frac{v_n}{2\pi|\mathbf{r}_{if}|} ds = v_n * \int_{S_i} \frac{\delta(t - |\mathbf{r}_{if}|/c)}{2\pi|\mathbf{r}_{if}|} ds_i = v_n * h(\mathbf{r}_f, t) \quad (8)$$

where v_n is the vibration velocity of transducer surface, c is ultrasound velocity in the medium, $|\mathbf{r}_{if}| = |\mathbf{r}_f - \mathbf{r}_i|$ is the distance from the source point located at \mathbf{r}_i to elementary areas of the flaw at \mathbf{r}_f , $h(\mathbf{r}_f, t)$ is the spatial impulse response of the transmit transducer at location \mathbf{r}_f .

The velocity of the transmitted ultrasound at the elementary areas of the flaw is given by

$$v_i(\mathbf{r}_f, t) = -\text{grad } \phi(\mathbf{r}_f, t) \quad (9)$$

where grad is the gradient operation.

The reflector velocity of the elementary areas of the flaw at \mathbf{r}_f is given by

$$v_f(\mathbf{r}_f, t) = -r_p(\mathbf{r}_{if}, \mathbf{n})v_n * \left(\frac{1}{c} \frac{\partial}{\partial t} h(\mathbf{r}_f, t) + \frac{1}{|\mathbf{r}_{if}|} h(\mathbf{r}_f, t)\right) \quad (10)$$

where $r_p(\mathbf{r}_{if}, \mathbf{n})$ is reflection coefficient of the transmitted ultrasound interacted with the flaw element, \mathbf{n} is normal vector of the flaw element.

The velocity of the transmitted ultrasound at the elementary areas of the receiving transducer is given by

$$\phi'(\mathbf{r}_r, t) = \cos(\mathbf{r}_{fr}, \mathbf{n})v_f(\mathbf{r}_f, t) * \int_{S_r} \frac{\delta(t - |\mathbf{r}_{fr}|/c)}{2\pi|\mathbf{r}_{fr}|} dS, \quad (11)$$

where $|\mathbf{r}_{fr}| = |\mathbf{r}_r - \mathbf{r}_f|$ is the distance from the flaw element located at \mathbf{r}_f to the receiving transducer elementary at \mathbf{r}_r , $\cos(\mathbf{r}_{fr}, \mathbf{n})$ is the cosine of the angle between the normal vector \mathbf{n} and vector \mathbf{r}_{fr} . The spatial impulse response of flaw element S' at \mathbf{r}_f is given by

$$h'(\mathbf{r}_{fr}, t) = \int_{S'} \frac{\delta(t - |\mathbf{r}_{fr}|/c)}{2\pi|\mathbf{r}_{fr}|} dS' \quad (12)$$

Eq.(11) can be rewritten as

$$\phi'(\mathbf{r}_r, t) = \cos(\mathbf{r}_{fr}, \mathbf{n}) v_f(\mathbf{r}_f, t) * h'(\mathbf{r}_{fr}, t) \quad (13)$$

The acoustic pressure over the surface of the receiving transducer is

$$p(\mathbf{r}_r, t) = \frac{1}{S_r} \int_{S_r} \int_{S_f} \rho \frac{\partial \phi'(\mathbf{r}_r, t)}{\partial t} dS_f dS_r \quad (14)$$

By substituting Eq.(10) and Eq.(13) in Eq.(14) and comparing with Eq.(4), The response of flaw is

$$h_s(t) = -\frac{\rho}{S_r} \frac{\partial}{\partial t} \int_{S_r} \int_{S_f} \cos(\mathbf{r}_{fr}, \mathbf{n}) r_p(\mathbf{r}_{fr}, \mathbf{n}) h'(\mathbf{r}_{fr}, t) * \left(\frac{1}{c} \frac{\partial}{\partial t} h(\mathbf{r}_f, t - |\mathbf{r}_{fr}|/c) + \frac{1}{|\mathbf{r}_{fr}|} h(\mathbf{r}_f, t - |\mathbf{r}_{fr}|/c) \right) dS_f dS_r \quad (15)$$

The spatial impulse response of flaw is

$$h_s(t) = -\frac{1}{S_r} \int_{S_r} \int_{S_f} \cos(\mathbf{r}_{fr}, \mathbf{n}) r_p(\mathbf{r}_{fr}, \mathbf{n}) h'(\mathbf{r}_{fr}, t) * \left(\frac{1}{c} \frac{\partial}{\partial t} h(\mathbf{r}_f, t - |\mathbf{r}_{fr}|/c) + \frac{1}{|\mathbf{r}_{fr}|} h(\mathbf{r}_f, t - |\mathbf{r}_{fr}|/c) \right) dS_f dS_r \quad (16)$$

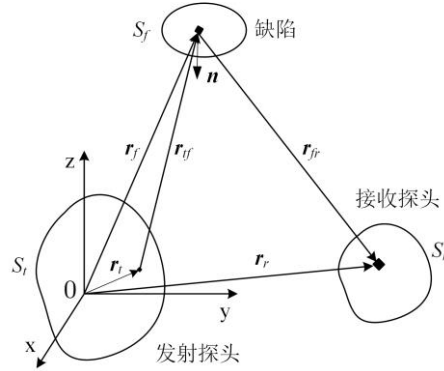


Fig.2 Schematic of flaw's impulse response

3 Results

3.1 Transducer response profile

A plane block test is used to calculate transducer response. The reflect echo from the back surface of the planar test block is acquired using a 2.5MHz, 20mm-diameter transducer excited with short pulse by a pulser/receiver(CTS-4020, SIUI, China), the thickness of plane block test is 40mm, the velocity of ultrasound transmitted in the block test is 5900m/s. The transducer is placed in a magnet-absorbing probe rob holder which is used to avoid problem due to variations in coupling.

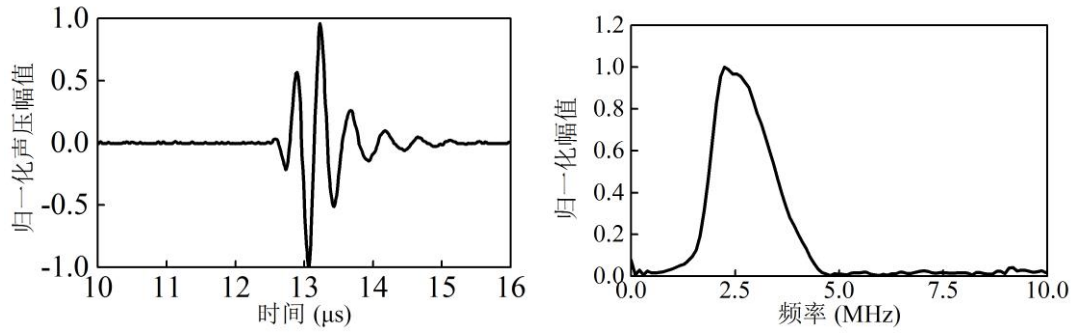


Fig.3 Reflect echo from the back surface of plane test block. (a): time-domain waveform; (b): amplitude spectrum of pulse echo

Using Eq. (15) one can calculate impulse response of flaw. For the modeling, the big plane test block is assumed as a 80mm-diameter reflector (the pressure on the edge element is 0.5% of the central point), the reflector is divided into 1×1 mm elements, the receiving transducer is divided into 0.5×0.5 mm elements. The impulse response of the reflector is represented in Fig.4, the presents results agreed well with the results in literature [19], the response of the reflector is represented in Fig.5.

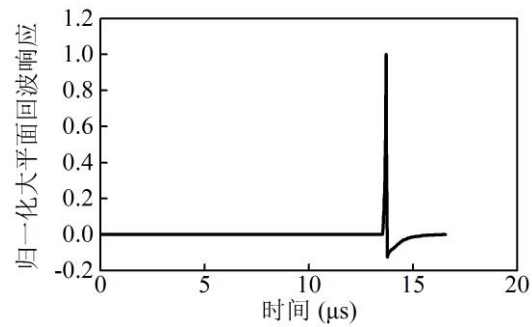
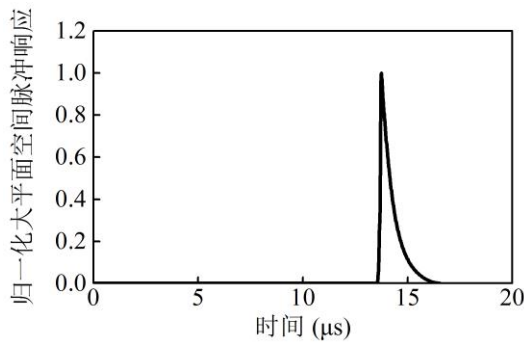


Fig.4 The impulse response of the plane test block. Fig.5 The response of the plane test block

Using Eq. (7) one can calculate the transducer response $v(t)$, the results is shown in Fig.6, and

$$Q^2 = 0.05 \max(|H_p(\omega)|^2).$$

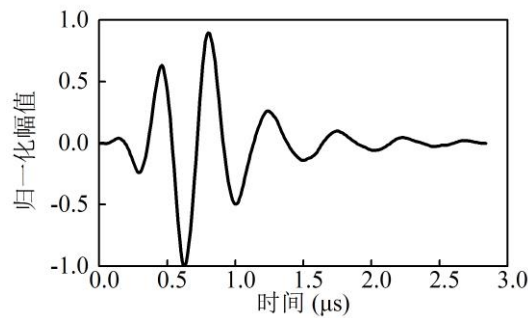


Fig.6 The transducer response

3.2 Simulation and measured results

Flat bottom hole (FBH) is commonly used in nondestructive testing to adjust the sensitivity and the AVG curve, it also can be used to simulate the crack defects. It's more difficult to inspect in-service components actually, the space placing transducer is narrow, the transducer is hardly right above the defects. So we designed two block to study characteristics of flaw impulse response of targets on and off-axis. Block diagram of the measurement setup is shown in Fig.7, thickness of the block is $T=65$ mm, diameter of the FBH is d , distance between FBH and transducer is L , diameter of the transducer is $D=20$ mm.

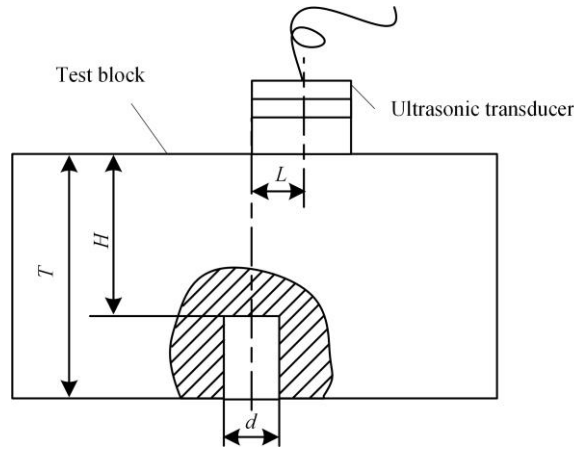
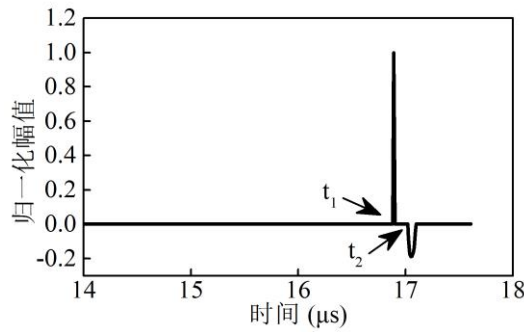
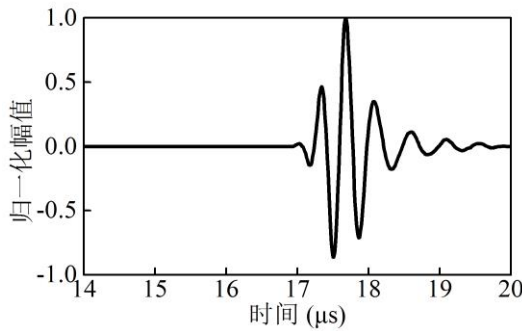


Fig.7 Block diagram of the measurement setup

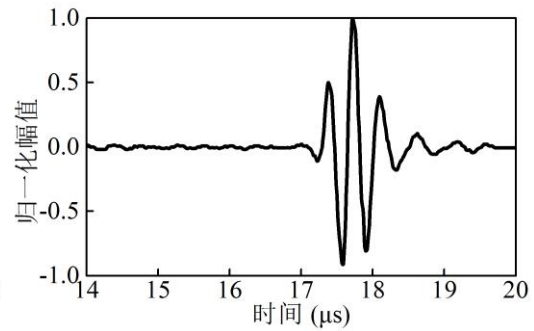
Fig.8 shows the comparison of experimental and theoretical signals in the case of $d=2\text{mm}$ and $L=0\text{mm}$, the amplifier has a 79dB voltage gain. All pressure amplitudes have been normalized by the maximum theoretical and experimental values. The impulse response of FBH is composed of two pulses, however, polarity is opposite, the first pulse at $t_1 = 16.89\mu\text{s} \approx 2H/c$ is far greater than the second pulse at $t_2 = 17.05\mu\text{s} \approx H/c + \sqrt{H^2 + (D/2)^2}/c$. The first pulse is called the direct wave component, the second pulse is called the edge wave component. Since the FBH and the probe is coaxial, all edge wave components arrive receiving transducer at the same time, duration of the edge wave is very short. The time difference of direct and edge wave is $0.16\mu\text{s}$, so direct wave overlaps with edge wave. It is verified that the computational method used in this work predicts accurately the theoretical and experimental signal, both qualitatively (shape of the echo waveform) and quantitatively (relative amplitude).



(a)



(b)

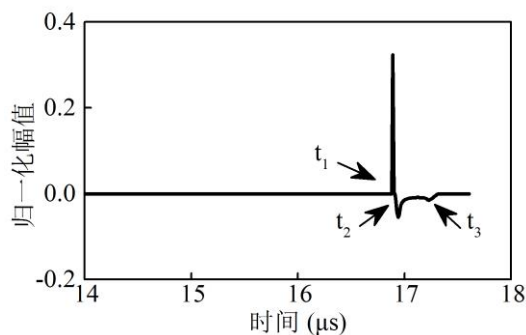


(c)

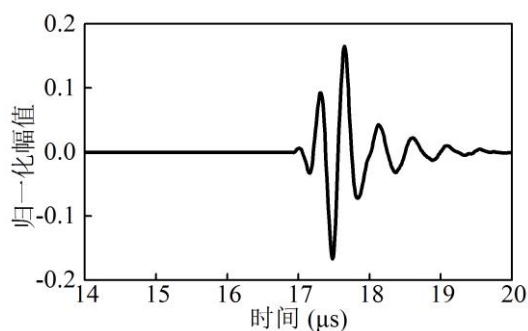
Fig.8 The comparison of experimental and theoretical signals in the case of $d=2\text{mm}$ and $L=0\text{mm}$, (a): impulse response of FBH; (b): theoretical signal; (c): experimental signal.

Fig.9 shows the comparison of experimental and theoretical signals in the case of $d=2\text{mm}$ and $L=5\text{mm}$, the amplifier has a 79dB voltage gain. All pressure amplitudes have been normalized by the maximum theoretical and

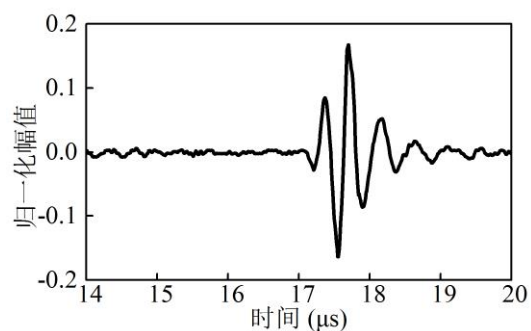
experimental values recorded for $L=0\text{mm}$. The impulse response of FBH is composed of three pulses, the first pulse is positive, the second and third pulse is negative. The first pulse at $t_1 = 16.89\mu\text{s} \approx 2H/c$ is far greater than two others. The second pulse at $t_2 = 17.05\mu\text{s} \approx H/c + \sqrt{H^2 + (D/2)^2}/c$ is the closet edge wave component, the third pulse at $t_3 = 17.38\mu\text{s} \approx H/c + \sqrt{H^2 + (3D/4)^2}/c$ is the farthest edge wave component. The amplitude at t_2 is larger than t_3 because the reflection coefficient is larger at t_2 .



(a)



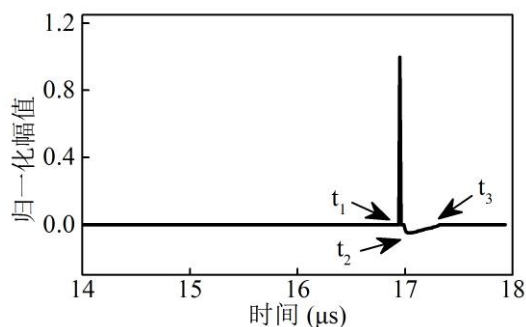
(b)



(c)

Fig.9 The comparison of experimental and theoretical signals in the case of $d=2\text{mm}$ and $L=5\text{mm}$, (a): impulse response of FBH; (b): theoretical signal; (c): experimental signal.

Fig.10 and Fig.11 show the comparison of experimental and theoretical signals of a 5mm-diameter-FBH in the case of $L=0\text{mm}$ and $L=5\text{mm}$, the amplifier has a 70dB voltage gain. The impulse response of FBH is composed of three pulses, the direct wave is major contribution. The greater off-axis distance, the longer duration time and the smaller amplitude. Compared with Fig.8 and Fig.9, the target size has an influence on the echo signal, the amplitude of the direct wave increases with the target diameter contrary to the edge wave.



(a)

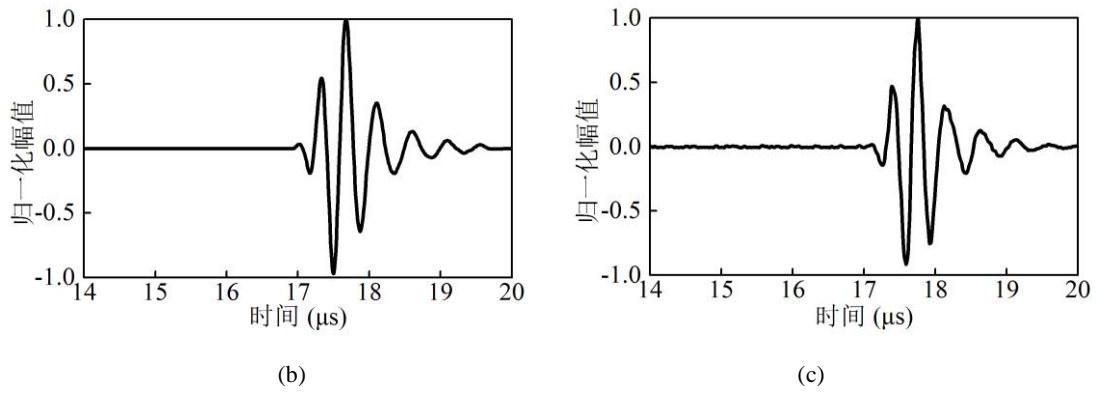


Fig.10 The comparison of experimental and theoretical signals in the case of $d=5\text{mm}$ and $L=0\text{mm}$, (a): impulse response of FBH; (b): theoretical signal; (c): experimental signal.

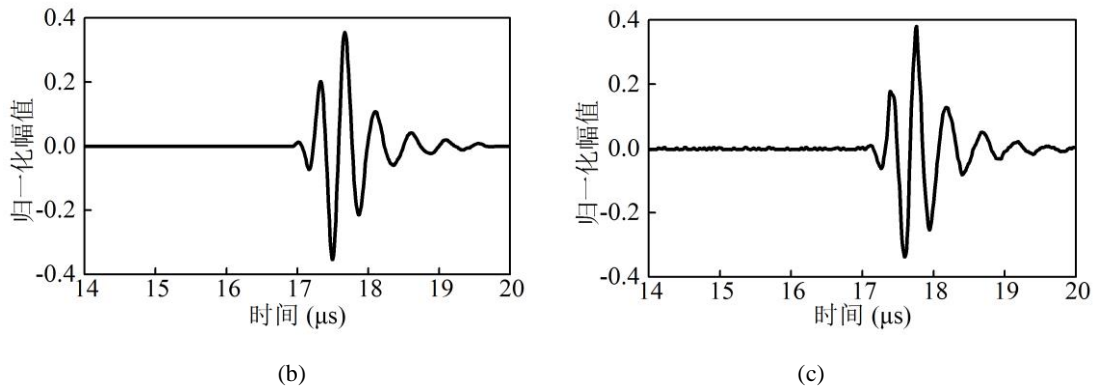
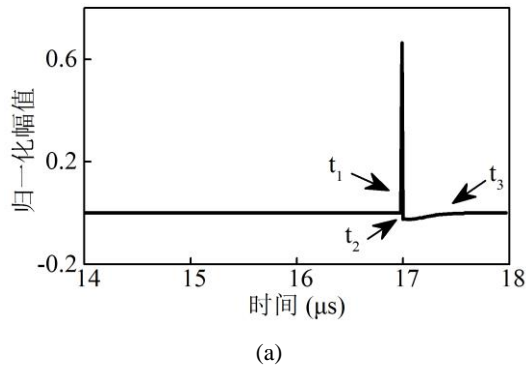


Fig.11 The comparison of experimental and theoretical signals in the case of $d=5\text{mm}$ and $L=5\text{mm}$, (a): impulse response of FBH; (b): theoretical signal; (c): experimental signal.

4 Conclusion

A model is proposed to predict the echo response from a plane defect based on the Huygens' principle of superposition. Spatial impulse response and Kirchhoff approximation are applied to model the interaction of the ultrasonic wave with flaws. The electromechanical response profile of transducer is calculated by deconvolution the echo of plane test block with impulse response of the test block. Characteristics of flaw impulse response of targets on and off-axis are analyzed in detail, the received ultrasonic echo is explained in terms of the plane and edge echoes, however, polarity is opposite. The amplitude of the direct echo is far greater than the edge echo. The target size has an influence on the echo signal, the amplitude of the direct wave increases with the target diameter contrary to the edge wave. The theoretically predicted results are in good agreement with the experimentally results.

References

- [1] Wu D, Li M X, Wang X M, et al. The ultrasonic transient field radiated by a normal shear wave probe. *Acta Acustica*, 2007; **32**(4): 304-309
- [2] Lyonnet F, Cassereau D, Cugnet M F. Parametric study of an ultrasonic non-destructive testing problem based on the reciprocity principle and a hybrid numerical method. *The Journal of the Acoustical Society of America*, 2015; **138**(3): 1939-1939.
- [3] Zhao X Y, Gang T, Zhang B X. An ultrasonic measurement model to predict the response from flat bottom hole for dual crystal contact probe[J]. *Acta Physica Sinica*, 2008; **57**(8): 5049-5055
- [4] Ghoshal G, Turner J A. Modeling of ultrasonic backscatter using ultrasonic radiative transfer theory. *The Journal of the Acoustical Society of America*, 2003; **114**(4):2357-2357
- [5] Guo X, Zhang D, Zhang J. Detection of fatigue-induced micro-cracks in a pipe by using time-reversed nonlinear guided waves: A three-dimensional model study. *Ultrasonics*, 2012; **52**(7): 912-919
- [6] Khelladi H, Djelouah H. The transducer vibratory profile effects on the detection of the transient ultrasonic field scattered by a rigid point reflector. *Ultrasonics*, 2010; **50**(4): 467-472
- [7] Nie X, Guo Z F, He Z C, et al. Parameters estimation of ultrasonic echo signal based on blind deconvolution and parameterized model. *Chinese journal of scientific instrument*, 2015; **36**(11): 2611-2616
- [8] Ye Z F, Li Y F, Jia F Y, et al. Study on the aging of the electronic properties of piezoelectric ceramic. *Journal of Lanzhou university(Natural sciences)*, 2001; **37**(3): 45-51
- [9] Buiochi F, Buiochi E B, Formigoni P O, et al. Computational method to determine reflected ultrasonic signals from arbitrary-geometry targets. *IEEE Transactions on Ultrasonics, Ferroelectrics and Frequency Control*, 2010; **57**(4): 986-994
- [10] Jensen J A. A model for the propagation and scattering of ultrasound in tissue. *The Journal of the Acoustical Society of America*, 1991; **89**(1):182-190
- [11] Szabo T L, Karbeyaz B Ü, Cleveland R O, et al. Determining the pulse-echo electromechanical characteristic of a transducer using flat plates and point targets. *The Journal of the Acoustical Society of America*, 2004; **116**(1): 90-96
- [12] Demirli R, Saniie J. Model-based estimation of ultrasonic echoes. Part I: Analysis and algorithms. *IEEE Transactions on Ultrasonics Ferroelectrics and Frequency Control*, 2001; **48**(3): 787-802
- [13] Boßmann Florian, Plonka Gerlind, Peter Thomas, et al.. Sparse Deconvolution Methods for Ultrasonic NDT. *Journal of Nondestructive Evaluation*, 2012; **31**(3): 225-244
- [14] Wei Liang, Huang Zuoying, Que Peiwen. Sparse deconvolution method for improving the time-resolution of ultrasonic NDE signals. *NDT and E International*, 2009; **42**(5): 430-434
- [15] Roberto H. Herrera, Eduardo Moreno, Héctor Calas and Rubén Orozco. Blind Deconvolution of Ultrasonic Signals Using High-Order Spectral Analysis and Wavelets. *Lecture Notes in Computer Science*, 2005; **3773**: 663-670
- [16] Jian X M, Li M X. Classification of flaw by adaptive filtering deconvolution of backscattering ultrasonic echo. *Acta Acustica*, 1999; **24**(6):637-644
- [17] Ping Wu, Stepinski, T. Spatial impulse response method for predicting pulse-echo fields from a linear array with cylindrically concave surface. *IEEE Transactions on Ultrasonics Ferroelectrics and Frequency Control*, 1999; **146**(5): 1283-1297
- [18] Zhang B X, Wang W L. Reflection and refraction on the fluid-solid interface of acoustic field excite b a concave phased array. *Acta Physica Sinica*, 2008; **57**(6):3613-3619
- [19] Rhyne T L. Radiation coupling of a disk to a plane and back or a disk to a disk: an exact solution[J]. *The Journal of the Acoustical Society of America*, 1977; **61**(2): 318-324

This work was supported by the National Natural Science Foundation of China (51074121), the China Postdoctoral Science Foundation (2015M572653XB), the Scientific Research Program Funded by Shaanxi Provincial Education Department(15JK1455) and the Key Laboratory of Expressway Construction Machinery of Shaanxi Province(310825161124)

Corresponding author: DONG Ming, E-mail: jesunatg@hotmail.com

联系方式:

董明, tel: 013310943653;

email:jesunatg@hotmail.com;

身份证号: 422828198408221517

地址: 陕西省西安市雁塔中路 58 号西安科技大学机械学院, 710054